Title

[FeFe]-Hydrogenase Maturation: Insights into the Role HydE Plays in Dithiomethylamine Biosynthesis

Journal

Biochemistry, 54(9)

ISSN

0006-2960

Authors

Betz, Jeremiah N
Boswell, Nicholas W
Fugate, Corey J
et al.

Publication Date

2015-03-10

DOI

10.1021/bi501205e

Peer reviewed

HHS Public Access

Author manuscript

Biochemistry. Author manuscript; available in PMC 2016 April 21.

Published in final edited form as:

Biochemistry. 2015 March 10; 54(9): 1807–1818. doi:10.1021/bi501205e.

[FeFe]-Hydrogenase Maturation: Insights into the role HydE plays in dithiomethylamine biosynthesis

Jeremiah N. Betz[†], **Nicholas W. Boswell**[†], **Corey J. Fugate**[†], **Gemma L. Holliday**[‡], **Eyal Akiva**[‡], **Anna G. Scott**[†], **Patricia C. Babbitt**[‡], **John W. Peters**[†], **Eric M. Shepard**[†], and **Joan B. Broderick**[†,*]

[†]Department of Chemistry & Biochemistry, Montana State University, Bozeman, MT 59717, United States

[‡]Department of Bioengineering & Therapeutic Sciences, University of California, San Francisco, CA 94158, United States

Abstract

HydE and HydG are radical *S*-adenosylmethionine enzymes required for the maturation of [FeFe]-hydrogenase (HydA) and produce the non-protein organic ligands characteristic of its unique catalytic cluster. The catalytic cluster of HydA (the H-cluster) is a typical [4Fe-4S] cubane bridged to a 2Fe-subcluster that contains two carbon monoxide, three cyanide, and a bridging dithiomethylamine as ligands. While recent studies have shed light on the nature of diatomic ligand biosynthesis by HydG, little information exists on the function of HydE. Herein, we present biochemical, spectroscopic, bioinformatics, and molecular modeling data that together map the active site and provide significant insight into the role of HydE in H-cluster biosynthesis. Electron paramagnetic resonance and UV-visible spectroscopic studies demonstrate that reconstituted HydE binds two [4Fe-4S] clusters and copurifies with *S*-adenosyl-L-methionine. Incorporation of deuterium from D_2O into 5'-deoxyadenosine, the cleavage product of *S*-adenosyl-L-methionine, coupled with molecular docking experiments suggests that the HydE substrate contains a thiol functional group. This information, along with HydE sequence similarity and genome context networks, have allowed us to redefine the presumed mechanism for HydE away from BioB-like sulfur insertion chemistry; these data collectively suggest that the source of the sulfur atoms in the dithiomethylamine bridge of the H-cluster are likely derived from HydE's thiol containing substrate.

Graphical abstract

Corresponding Author. Joan B. Broderick, (406) 994-6160, jbroderick@chemistry.montana.edu.

ASSOCIATED CONTENT

Supporting Information

D-atom incorporation into dAdoH and putative substrate structures, additional EPR spectra that include temperature relaxation and power saturation data, table of simulated g-values, and genomic context network diagram. This material is available free of charge via the Internet at http://pubs.acs.org.

Author Contributions

The manuscript was written through contributions of all authors. All authors have given approval to the final version of the manuscript.

No competing financial interests have been declared.

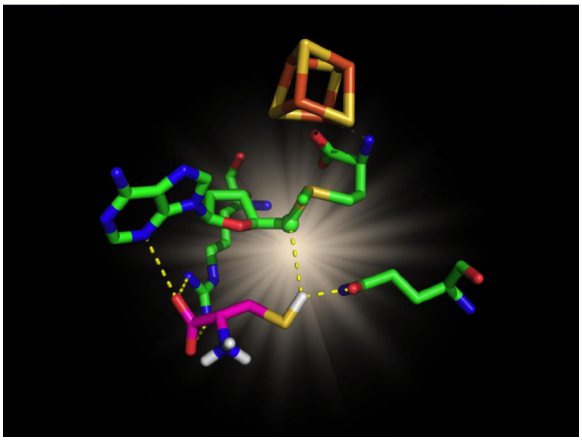

Keywords

radical SAM; hydrogenase; maturase; HydE; dithiomethylamine; thiol; iron; sulfur; AdoMet

The interconversion of H_2 to $2H^+$ and $2e^-$ within microoganisms is catalyzed by the [FeFe]- and [NiFe]-hydrogenases.[1] Despite a lower tolerance for O_2, [FeFe]-hydrogenase is the more promising catalyst for economical hydrogen production due to its higher turnover rates that are on the order of 10^4 turnovers per second.[2–4] [FeFe]-hydrogenases (HydA) contain a catalytic 6Fe-cluster, termed the H-cluster, which through biochemical, analytical, spectroscopic, and crystallographic investigations was found to contain a [4Fe-4S] cluster bridged by a cysteine thiolate to a uniquely decorated 2Fe-subcluster (Figure 1).[5–7] The two irons of the subcluster are bridged by one carbon monoxide and a dithiomethylamine (DTMA) ligand. Each iron is additionally coordinated by one carbon monoxide and one cyanide.

An intriguing clue to H-cluster assembly was provided when analysis of insertional mutants revealed that two putative radical *S*-adenosylmethionine (SAM) enzymes were necessary for maturation of HydA.[8] These radical SAM enzymes, HydE and HydG, both contain the CX_3CX_2C motif characteristic of this enzyme superfamily, and both have been shown to coordinate a [4Fe-4S] cluster at this motif.[9] HydG utilizes radical SAM chemistry to cleave tyrosine to produce *p*-cresol, CO and CN^-; the diatomics are subsequently incorporated into the 2Fe-subcluster component of the H-cluster of HydA.[10–13] The role of HydE is undefined and the topic of the current study. A third protein required for HydA maturation, HydF, is a GTPase that binds iron-sulfur clusters and appears to serve as a scaffold or carrier for assembly and delivery of the 2Fe-subcluster of the H-cluster.[14–17]

While biochemical and structural studies of HydE have confirmed its assignment as a radical SAM enzyme with a complete TIM barrel $(\beta\alpha)_8$ structure, no direct insight into its role in maturation has yet been provided.[9, 18, 19] Because synthesis of the diatomics is accomplished by HydG[11, 14], and scaffolding of the 2Fe precursor is carried out by HydF[14, 20], it is presumed that HydE functions in DTMA synthesis.[21, 22] While it was previously proposed that the DTMA bridge could be derived from tyrosine[10], a recent spectroscopic study of HydA matured in the presence of ^{15}N-tyrosine ascribes the

bridgehead atom of the DTMA bridge to a source other than tyrosine.[23] HydE was originally hypothesized to catalyze biotin synthase-like sulfur insertion chemistry,[9] however, it has more recently been observed that HydE shares significant sequence similarity to methylornithine synthase (PylB).[24] This homologous relationship perhaps points to a different type of radical SAM reaction for HydE.[25] Sequence percent identities between HydE and related proteins have been previously described in literature[26] and a sequence alignment is in Figure S1

In this study, we present data showing that select low-molecular weight thiol containing compounds significantly increase the rate of HydE catalyzed SAM cleavage and also promote incorporation of deuterium from D_2O into the SAM cleavage product 5'-deoxyadenosine (dAdoH). Molecular docking investigations place several of these thiols, including D/L-cysteine, D/L-homocysteine, mercaptopyruvate, γ-glutamylcysteine, and dithiothreitol, within the active site, such that the thiol hydrogens are positioned appropriately for direct abstraction by the dAdo• that would be generated upon reductive cleavage of SAM. The results help to define the chemical properties of the HydE substrate and indicate that it contains a thiol functional group that is located approximately 5 Å from the 5' position of SAM. These clues lead us to a proposed mechanism for synthesis of the DTMA bridge of the H-cluster involving small molecule lyase activity that is reminiscent of HydG chemistry. Together, our results shift the HydE paradigm away from that of BioB-like sulfur insertion chemistry and towards the premise that the DTMA sulfur atoms of the 2Fe subcluster are derived from HydE's substrate.

Experimental Procedures

Cloning, cell growth, and expression

The *Clostridium acetobutylicum* gene *hydE* was cloned into Novagen® pET-23b vector utilizing the *Nde*I and *Xho*I restriction sites from a previously characterized *C. acetobutylicum hydE* construct.[20] Sequence verified constructs were transformed into Agilent Technologies BL21-CodonPlus®(DE3)-RIL competent cells and used to express recombinant *C. acetobutylicum* HydE with a C-terminal poly-His tag. Cells were grown and harvested using procedures adapted from a previously published method.[14] Cultures in phosphate buffered LB were grown to an OD_{600} of 0.5 after which they were induced with 1 mM IPTG (final concentration), supplemented with 0.3 mM $(NH_4)_2Fe(SO_4)_2{\cdot}6H_2O$, and incubated aerobically for 2.5 hrs. After room temperature equilibration, the cultures were sparged with N_2 at 4 °C for 14 hrs. The wet cell paste, pelleted by centrifugation, was flash frozen in liquid nitrogen and stored at −80 °C.

Purification and reconstitution of HydE

All purification and reconstitution steps were carried out in an anaerobic Coy chamber (Grass Lakes, MI) containing a 2–4% hydrogen in nitrogen atmosphere in a 4 °C cold room. The stock buffer contained 25 mM HEPES pH 8.0, 0.5 M KCl, and 5% glycerol (w/v) unless otherwise specified. Cells were lysed using procedures similar to those previously described[20] with a lysis buffer cocktail containing the stock buffer supplemented with 10 mM imidazole, lysozyme, 1% Triton X-100, PMSF, DNase I, and RNase A. HydE protein in

the clarified lysate was captured by Qiagen® Ni-NTA resin in a gravity flow column. Bound protein was washed with 10 mM imidazole followed by 25 mM imidazole prior to elution with 250 mM imidazole all in the stock buffer. Colored fractions were pooled and then either dialyzed or buffer exchanged into the stock buffer to remove imidazole prior to flash freezing and storage at −80 °C.

Reconstitution of HydE was accomplished using previously published techniques.[14] Briefly, HydE was supplemented with 5 mM DTT, followed by a 6-fold excess of $Na_2S{\cdot}9H_2O$ and $FeCl_3$. This mixture was incubated for 2 hours prior to centrifugation to remove FeS particulates; the clarified protein was then buffer exchanged with a Sephadex G25 resin column to remove adventitiously bound iron, sulfide, and DTT. The protein was concentrated using Amicon 10 kDa molecular weight cut-off filters (Millipore) and flash frozen in liquid N_2 for biochemical and spectroscopic characterization. Bradford assays were utilized for protein quantitation using a BSA standard solution. The iron content of purified HydE was determined using a ferrozine colorimetric assay.[27]

EPR and UV-Vis spectroscopic characterization

Samples were prepped in an MBRAUN chamber ($O_2 \leq 1$ ppm) using reagents degassed on a Schlenk line. HydE samples for EPR characterization (200 μL final volume) were prepared using two batches of reconstituted protein of 160 and 275 μM concentrations with 7.6 ± 0.1 and 8.2 ± 0.2 irons per protein, respectively. Two methodologies were utilized for preparation of reduced HydE. The first employed incubation of as-reconstituted enzyme with 4 mM dithionite for 1 min prior to adding SAM; samples were rapidly mixed and then flash frozen in liquid N_2. The second technique relied on addition of 5-deazariboflavin (100 μM final concentration) to as-reconstituted enzyme; samples were photoreduced when illuminated in the presence of 50 mM Tris for 1 hour in an ice water bath by using a 500 W T3 halogen bulb.[28]

Low temperature, continuous wave X-band spectra were recorded on a Bruker ER-200D-SRC spectrometer equipped with a liquid helium cryostat and temperature controller (Oxford instruments). EPR parameters, unless otherwise noted, were: microwave frequency, 9.37 GHz; temperature, 12 K; power, 1 mW; time constant/conversion time, 20.48 msec; receiver gain, 1×10^4; modulation frequency, 100 kHz; and modulation amplitude, 10 G. Experimental spectra were baseline adjusted using OriginPro (Version 8.5) and reported g-values were assigned by simulation using the EasySpin 4.5.0 software program.[29]

The UV-Vis absorption spectroscopy of proteins and small molecules was carried out on samples in 1.4 mL anaerobic cuvettes (Spectrocell) using a Varian Cary 6000i UV-vis/near IR spectrophotometer.

SAM cleavage assays

All enzymatic assays were conducted under anaerobic conditions in an MBRAUN glove box ($O_2 \leq 1$ ppm). SAM was prepared enzymatically using crude SAM synthetase lysate by a previously described method.[30] HydE (25 μM final concentration) was incubated with 0.5 mM (final concentration) SAM and putative substrates (2.5 mM final concentration). Reactions were initiated with addition of sodium dithionite (2 mM final concentration) and

at select time points assay aliquots (45 μL) were quenched by addition of 400 mM acetic acid, pH 4.5 (5 μL). Quenched aliquots were incubated on ice for approximately 1 hr prior to centrifugation for 10 min at 4 °C.

Quantitation of 5'-deoxyadenosine (dAdoH) was accomplished with an Agilent Technology 1100 series HPLC. Mobile phase solvent A was H_2O, while solvent B was acetonitrile; both solvents contained 0.1 % acetic acid. Assay supernatants (10 μL) were injected onto a Phenomenex Kinetex 5u PFP 100A column equilibrated in 2.0 % solvent B. The column was washed with 2.0 % solvent B for 3.3 min and then a linear gradient was initiated up to 60 % solvent B at 11 min; dAdoH eluted at 6.8 min as determined by HPLC of a standard solution, and was observed as a sharp absorbance peak at 254 nm. Analysis was performed using peak integration by ChemStation software, and unknowns were compared to a dAdoH standard curve for quantitation.

Analysis of deuterium incorporation into dAdoH and SAM

In order to probe incorporation of substrate-derived deuterium into either dAdoH or SAM during HydE catalysis, a series of assays were constructed to monitor the isotopic mass distributions of dAdoH and SAM. These assays were conducted in a manner similar to that described above, but reaction time point aliquots (20 μL) were first quenched with 60 μL of acetone, then centrifuged to remove precipitated protein, and further diluted 5-fold by addition of 50:50 acetone:H_2O prior to LC/MS injection. For assays to examine H-atom abstraction from solvent exchangeable positions on putative substrate molecules, assays were run in D_2O buffer that was prepared by two sequential rounds of the stock H_2O buffer dessicated on a Schlenk line subsequently rehydrated in D_2O (99.8 % D). L-cysteine-2,3,3-d_3 from Cambridge Isotope Laboratories was 98 % D.

Following injection of sample (2 μL), assay components were separated using an Agilent Technologies 1200 series HPLC with normal phase chromatography on a Cogent Diamond Hydride 100A 4 μm 150 × 2.1 mm column. Mobile phases A and B were water and acetonitrile, respectively, and both contained 0.1 % TFA. The loaded column was washed with 100 % solvent B for 1 min, and solutes eluted during a linear gradient from 100 % to 50 % solvent B over the next 5 min. Mass spectrometry was performed downstream with an Agilent 6538 UHD Accurate-Mass QTOF LC/MS in positive mode. Extracted ion chromatograms of m/z values 252.106 (3.5 min) and 399.140 (6.5 min) principally corresponded to the dAdoH + H^+ and SAM + H^+, respectively. Agilent Qualitative Analysis B.04.00 of the MassHunter software suite was used to determine the isotopic distributions of dAdoH and SAM. Deuteration of dAdoH did not affect the retention time in the column as the 252, 253, and 254 m/z peaks temporally overlaid in the mass chromatogram. After initially locating the dAdoH+H^+ signals from an extracted ion chromatogram (EIC) at 252.108 m/z, the bins (1 sec) surrounding the center of the EIC peak with quantifiable isotopic peaks containing at least 252 and 253 m/z were selected for quantitation. The 252, 253, and 254 m/z peak areas were quantitated using the raw total ion chromatogram at the selected retention time range. The relative incorporation of deuterium was calculated by dividing the 253 m/z area with that of the 252 m/z area. The isotopic ratio of dAdoH synthesized from natural abundance reagents used for standard curves (H_2O) was 0.121

± 0.002, and is very close to the theoretical ratio of 0.130. Isotopic distributions of SAM and dAdoH with an additional proton were calculated using an isotopic distribution calculator from Scientific Instrument Services (sisweb.com).

Molecular docking experiments

Molecular docking was performed with Autodock 4.2.[31] Ligand coordinates were prepared using Avogadro.[32] The structure of HydE from *Thermotoga maritima* was obtained from Protein Data Bank (PDB ID 3IIZ). HydE was prepared for docking by removing all bound water molecules and ligands with the exception of *S*-adenosyl-L-methionine. Polar hydrogens were added using Autodock Tools.[31] "Blind docking" of the various ligands was performed against HydE using a box that enclosed the solvent accessible area of the barrel. The size of the grid box was 60 Å × 60 Å × 60 Å with center x, y, z at 45, 3, 18. A Lamarckian genetic algorithm was used to generate 100 bound conformations for the ligand. All other settings were kept as default.

Construction of sequence similarity and genomic context networks

Sequence similarity networks were obtained from the Structure-Function Linkage Database (SFLD).[33] A cartoon was manually generated depicting the subgroup context in which HydE family sequences and those of its most similar reaction families are found.

Genomic context networks, representing an orthogonal approach to substrate docking or inference from HydE homologous proteins, were employed to study the genomic context of these enzymes. Since there are many cases in which HydE enzymes are encoded within a gene neighborhood comprising other components of the H-cluster biosynthetic pathway (*hydAFG*), other conserved gene neighbors may encode enzymes also involved in the pathway and potentially biochemically associated with HydE catalysis. To this end, a genomic context network approach was utilized, similar to the one described in Zhao *et al.*[34] Each of the 563 HydE family enzymes was mapped onto its corresponding genome, and the ten proteins encoded upstream and downstream were gathered (as established in the ENA database[35]) creating a set of ~7,000 gene neighbors. A sequence similarity network of all these proteins was then created using Pythoscape.[36] All proteins were subsequently annotated based on data retrieved from UniProtKB[37] and the minimal pairwise similarity for similarity inclusion was determined by sampling and inspecting different thresholds, with the aim of finding the best compromise between network clusters and functional annotation. The optimal threshold of pair-wise BLAST E-values was set to be $1e^{-20}$. Upon ranking the different clusters in the network, the largest clusters displaying the widest phylogenetic distribution were analyzed to provide clues about the mechanism of HydE.

Results

Spectroscopic characterization of HydE

Anaerobically purified *C. acetobutylicum* HydE typically contains 2 – 4 irons per protein. Substoichiometric cluster loading is typical for radical SAM enzymes[14] and therefore we introduced a chemical reconstitution step prior to further characterization. Reconstitution of recombinant HydE with exogenous iron and sulfide under reducing conditions caused the

intensity of the LMCT features at 420 nm to increase 2.2-fold (Figure 2). Using published extinction coefficients at 410 nm[38] and 420 nm[39, 40] for proteins with [4Fe-4S] clusters (15,000 – 17,000 ($M^{-1}cm^{-1}$) per [4Fe-4S] cluster), the iron loading for as-purified *C. acetobutylicum* HydE was calculated to be 3.5 Fe/protein, in good agreement with the value of 3.7 Fe/protein obtained from the colorimetric iron assay. Likewise, after reconstitution the iron numbers determined using either published extinction coefficients or results of the colorimetric iron assay were in excellent agreement (7.9 Fe/protein and 8.6 Fe/protein, respectively). Three independent purification and reconstitution events of HydE used for turnover assays showed that the enzyme averaged 8.1 ± 0.5 Fe/protein. Based on the presence of eight cysteine residues in the primary sequence, this iron number is indicative of full loading of two [4Fe-4S] clusters (Figure 2).

Low temperature EPR spectroscopy shows that as-reconstituted HydE exhibits a nearly isotropic signal that both temperature relaxation profiles (Figure S3C) and simulations (Figure 3A) show arises from two independent signals centered at g = 2.01 and g = 2.00 (composite 0.02 spin/protein). The first of these signals likely arises from a $[3Fe\text{-}4S]^{+}$ cluster given its fast temperature relaxation profile.[41] We assigned the second signal to that of a $[2Fe\text{-}2S]^{+}$ cluster, given its maximum signal intensity at around 30 K.[14] Both these cluster types are likely present due to either partial [4Fe-4S] cluster degradation or incomplete reconstitution (Figure S3C). In addition to the signals in the g ~ 2 region, broad field spectra (Figure S3A) of as-reconstituted protein show the presence of a minor spectral feature at g = 4.3 arising from high spin ferric iron adventitiously bound to the protein.

Reduction of as-reconstituted HydE with either sodium dithionite or 5-deazariboflavin (DRF) resulted in EPR spectra characteristic of reduced $[4Fe\text{-}4S]^{+}$ clusters accounting for 0.53 and 0.69 spins/protein, respectively (Figures 3B and S3B). Treatment of reduced HydE with SAM resulted in an intensification of the reduced signals (to 1.2 and 0.87 spins/protein for dithionite (Figure 3C) and DRF (Figure S3B), respectively). Temperature relaxation profiles for reduced HydE EPR signals both in the absence and presence of SAM show fast relaxation typical of $[4Fe\text{-}4S]^{+}$ clusters (Figure S4). Moreover, power dependence profiles reveal that the signals are largely resistant to saturation, consistent with their assignment to $[4Fe\text{-}4S]^{+}$ clusters (Figure S4).[42] Simulations of experimental data show that the EPR spectra for reduced samples are a composite of a three spin system that assign to SAM-bound and unbound N-terminal $[4Fe\text{-}4S]^{+}$ clusters, in addition to a C-terminal $[4Fe\text{-}4S]^{+}$ component (Figure 3B). The simulations reveal that the cluster signals attributed to the SAM-unbound states exhibit similar g values (g = 2.04, 1.92, 1.90 and g = 2.03, 1.91, 1.87); the g-values for the SAM-bound (presumably N-terminal) cluster underscore the perturbations induced by SAM coordination (g = 2.01, 1.88, 1.83). Moreover, simulations demonstrate that when exogenous SAM is added to reduced HydE, the resulting experimental spectra are well fit to a two spin system consisting of the SAM coordinated N-terminal $[4Fe\text{-}4S]^{+}$ cluster and the C-terminal $[4Fe\text{-}4S]^{+}$ cluster (Figure 3C). Table S1 lists the g-values obtained from spectral simulations for the data presented in Figure 3.

SAM copurifies with HydE

Both dithionite-treated and photoreduced samples of HydE (Figures 3 and S3B) have spectra that can be simulated using a combination of unbound $[4Fe\text{-}4S]^+$ and SAM coordinated $[4Fe\text{-}4S]^+$ cluster signals, even in the absence of added SAM. Based on normalization and spectral subtraction of the SAM-bound component from the spectrum of dithionite-reduced *C. acetobutylicum* HydE, approximately 25% of purified HydE contains SAM bound. In support of this observation, a SAM cleavage assay using 25 μM as-reconstituted HydE was performed in the absence of exogenous SAM and in the presence of coenzyme M; results showed that the amount of dAdoH reached a maximum concentration of 3.5 μM after 30 min. This indicates that at least 14% of the protein copurifies with SAM. This is likely a low estimate, as abortive cleavage of SAM is also known to produce methylthioadenosine (MTA), a product that was not quantified in these studies.[28] Additionally, the enzyme stock that was assayed underwent chemical reconstitution and gel filtration after purification, which may have removed some of the SAM that copurified HydE. Similarities exist between the unbound $[4Fe\text{-}4S]^+$ cluster signal we observe herein and the axial signal reported for reconstituted, reduced *Thermatoga maritima* HydE, although the latter exhibited low and high field shoulders.[9] While Rubach *et al.* attributed these shoulders to an accessory FeS cluster,[9] our analysis of *C. acetobutylicum* HydE suggests they instead likely arose from the coordination of SAM to the N-terminal, radical SAM cluster.

Substrate derived deuterium atom incorporation into deoxyadenosine

Given the observation that [FeFe]-hydrogenase maturation could be stimulated upon addition of L-cysteine,[43] we explored the possibility that this molecule may be a substrate for HydE by using deuterium-labeled cysteine and monitoring for D-atom incorporation into dAdoH and SAM. Deuterium atom incorporation into dAdoH was monitored by LC/MS by quantifying the ratio of peaks at m/z = 253 and 252; the ratio for dAdoH produced by HydE in the absence of cysteine in H_2O containing buffer was calculated to be 0.121 ± 0.002. In the presence of L-cysteine-2,3,3-d_3 (Figures 4A and S2), the 253/252 ratio was 0.120 ± 0.001, indicating that dAdo• did not abstract from either deuterated position. Assays were also performed in D_2O to test if a solvent exchangeable hydrogen on L-cysteine was abstracted by dAdo•; results from several assays show that the 253:252 peak ratios for L-cysteine increase from ~0.15 (no cysteine) to 0.43 ± 0.06 in the presence of cysteine (Figures 4A and S2), demonstrating that dAdo• abstracts a solvent-exchangeable hydrogen. While this H-atom abstraction could be occurring from a solvent-exchangeable position on the protein itself, the fact that appreciable D incorporation into 5'-deoxyadenosine is observed only in the presence of cysteine argues that the abstraction is occurring from cysteine.

Similar experiments were carried out with L-Ser, L-Ala, D-Cys, and L-homocysteine (L-Hcy) in D_2O, and revealed the importance of the thiol functionality. L-Ser and L-Ala lack the thiol but retain the amino and carboxylate functionalities; assays performed in their presence led to no detectable deuterium incorporation. Assays conducted with D-Cys and L-Hcy, on the other hand, resulted in similar D incorporation as observed with L-Cys (Figures 4A and S2). Mercaptopyruvate, glutathione (GSH), γ-L-glutamyl-L-cysteine (biosynthetic precursor of glutathione), 3-mercaptopropionic acid (3-MPA), and coenzyme M were also

examined as they all have possible biological significance and could be used to probe the size of the active site. Cysteamine, dithiothreitol (DTT), and β-mercaptoethanol (βME), while not biologically relevant, were also assayed to further investigate how charge plays a role in substrate binding. Other small molecules were also tested and are included in the summary that follows. From this set of experiments, the small molecules can be roughly divided into four groups based on their effect on D-atom incorporation from D_2O into dAdoH. L-Ala, L-Ser, GSH, pyruvate, and coenzyme A had a negligible stimulatory effect on D-atom incorporation into dAdoH. Cysteamine and γ-L-glutamyl-L-cysteine (γGC) stimulated very low level D incorporation, while L-homocysteine, L-cysteine, D-cysteine, mercaptopyruvate, DTT, and βME produced moderate incorporation of D into dAdoH. Coenzyme M and 3-mercaptopropionic acid produced the highest quantities of D-atom incorporation, with the dAdoH 253/252 ratios measured at 2.10 ± 0.33 and 2.16 ± 0.12, respectively. The isotopic m/z ratio (400/399) for SAM remained unchanged from natural abundance in all assays, indicating that the deuterated dAdoH was not subsequently converted to SAM (data not shown).

Deoxyadenosine production in the presence of select small molecules

In the absence of exogenous small molecules but in the presence of reducing agent, we calculated that *C. acetobutylicum* HydE catalyzes uncoupled SAM to produce dAdoH on the order of 1 turnover per HydE per hour, similar to a previously reported rate for *T. maritima* HydE.[9] All 20 common amino acids, pyruvate, and fumarate were screened for effects upon HydE dAdoH production. From these initial screens, only cysteine had any effect on SAM cleavage. Several mercaptans that stimulated D-atom incorporation into dAdoH were screened for their ability to increase dAdoH production (Figure 5). Stimulation of dAdoH production concurrent with D-atom incorporation is consistent with known radical SAM enzymes in the presence of substrates and substrate analogs.[10, 44] L-cysteine (3-fold increase), mercaptopyruvate (4-fold increase), coenzyme M (8-fold increase), and 3-mercaptopropionic acid (9-fold increase) all stimulate dAdoH production (Figure 5). Increased rates of dAdoH production for the thiols were consistent over 5.5 hours in assays, after which SAM became the limiting reagent in the reaction.

Molecular docking studies of putative HydE substrates and analogs

The x-ray crystal structure from *T. maritima* HydE (PDB ID 3IIZ) was utilized to perform *in silico* docking studies with the small molecules shown in Figure S2. The AutoDock software suite was selected for these studies given its precedence for predicting substrate and ligand binding sites.[45–47] All molecules containing either a carboxylate or sulfonate functional group were found to dock within the HydE active site adjacent to SAM with higher binding affinities than anywhere else inside or outside of the protein (Figure 6). The docked structures show that the small molecules are bound within a pocket comprising Arg159, the backbone nitrogens of Thr269 and Ala270, and the N3 nitrogen from the adenosyl group of SAM; these residues appear to play a critical role in stabilizing molecules with carboxylate/sulfonate groups. Moreover, the salt bridge formed by the guanidinium group of Arg159 and the negatively charged functional groups of the docked molecules appears to help position the thiols of the small molecules at distances (< 5 Å) amenable to H/D abstraction by the deoxyadenosyl radical (Figure 4B).[13] The binding energies for several small molecules are

tabulated in Figure 6. The opposite side of the putative substrate binding pocket contains the amide functional group of Gln107; this amide group is positioned only 4.2 Å from the 5' carbon of SAM. As the *in silico* modeling results show, this short distance would allow for hydrogen bonding between Gln107 and the solvent exchangeable, thiol hydrogen at a distance < 4 Å (Figure 6). In essence, Gln107 and the binding pocket that includes Arg159 appear to act as substrate handles for a variety of low molecular mass thiols, positioning these molecules in close proximity to SAM and thereby explaining the stimulatory effects in SAM cleavage and D-atom incorporation into dAdoH reported herein.

Radical SAM sequence similarity networks

While sequence similarity together with the similarity between the presumed dithiol product of HydE and the thiophane product of BioB led to the initial hypothesis that HydE could be involved in a sulfur insertion reaction during H-cluster biosynthesis.[48] Recent biochemical and crystallographic investigations into other structurally similar enzymes such as methylornithine synthase (PylB) and HydG leave room for a wide range of potential HydE chemistries.[11, 14, 24] The high degree of structural parallels between HydE and PylB (Figure 7B) reveals the overlap in the global protein armature, and also the prominent similarities in the two active site regions (Figure 7B).[24]

One additional tool to gain insight into the HydE substrate and reaction mechanism is analysis of Sequence Similarity Networks (SSN). The Structure-Function Linkage Database (SFLD) has identified nearly 100 thousand putative radical SAM enzyme sequences that may be categorized by their primary amino acid sequence.[33] Comparable sequences that likely exhibit the same function are grouped into nodes and adjacent nodes may be both structurally and functionally similar. As Figure 7A highlights, the other characterized radical SAM enzymes closest to HydE include PylB, HmdB, HydG, ThiH, NosL/NocL (3-Me), and BioB enzymes that are either predicted to or have been confirmed to contain complete TIM barrels $(\beta\alpha)_8$ and have small substrates that are less than 250 daltons.[25]

Genome context analysis

Based on genome context networks, gene clusters in Figure 8 and S5 represent the most conserved genes that are encoded near HydE enzymes from diverse phylogenetic origins. The largest and most phylogenetically diverse clusters turned out to be enriched with functions that typify HydF, HydG and TM1266 proteins (plurality vote using GO biological process annotation[49]), which are the known components of the H-cluster biosynthesis gene neighborhood; the genome context network captures other relevant pathway members, and we can accordingly have confidence that this analysis may offer clues about the HydE mechanism. The next clusters of highest rank are the ones annotated as AspA enzymes, cysteine syntheses, Cys/Met PLP-dependent enzymes and histidine kinases. The conservation of these HydE gene neighbors further supports the hypotheses involving cysteine in HydE's catalytic reaction.

Discussion

HydE cluster characteristics

Iron analysis of reconstituted *C. acetobutylicum* HydE, UV-vis extinction coefficients, and EPR temperature relaxation and power saturation characteristics indicate that protein used herein contains two fully loaded [4Fe-4S] clusters. A recent crystal structure revealed a second [4Fe-4S] cluster in reconstituted *T. maritima.* HydE,[50] consistent with our findings for the *C. acetobutylicum* protein. One cluster binds the radical SAM motif (CX_3CX_2C) in the N-terminal region of the protein and is absolutely conserved in HydE. The accessory CX_nCX_mC motif is only partially conserved and substitutions at these three cysteines do not impair [FeFe]-hydrogenase activation.[18] The second cluster of HydE likely plays no direct role in H-cluster biosynthesis. Given the high lability of the auxiliary cluster, as judged by the oxidation products observed in *T. maritima* HydE crystal structures,[50] this cluster may act as a sacrificial anode by reacting with external oxidants before they can damage the catalytically essential radical SAM [4Fe-4S] cluster.

Putative HydE substrates define the active site

Despite multiple solved X-ray crystal structures, insight into the substrate and reaction mechanism of HydE remains limited.[18, 19, 50] When assaying purified HydE with the 20 common amino acids, we observed a stimulatory effect on SAM cleavage/dAdoH production with L-cysteine (data not shown). Stimulation of SAM cleavage to produce dAdoH upon addition of substrate is a common characteristic of radical SAM enzymes and has been used, for example, to identify tyrosine as the substrate for HydG.[10, 25] The location of H-atom abstraction from putative substrates can be identified through use of selectively deuterated molecules. While L-cysteine-2,3,3-d_3 did not change the isotopic ratio of dAdoH (252/253 ratio) from that of natural abundance, addition of L-cysteine to HydE assays in D_2O did result in a shift in the dAdoH isotopic ratio. Interestingly, when testing a battery of small molecules, two trends emerge. First, the thiol functional group appears to be important for observing deuterium incorporation into dAdoH. Second, there is an upper limit on the size of thiol that can produce altered isotope ratios, presumably due to a size limit for fitting in to the HydE active site. Coenzyme A, glutathione, and γ-L-glutamyl-L-cysteine show little to no increase in dAdoH 253/252 isotopic ratio, suggesting that the natural substrate of HydE is smaller than these molecules. In addition to the size limitation and thiol functionality, a negative or partial negative charge appears to be important, as cysteamine has only a marginal effect despite its small size and thiol functional group.

Coenzyme M shows the largest stimulatory effect on both dAdoH production and D-atom incorporation into dAdoH, however coenzyme M cannot be the natural substrate of HydE because lysate activation experiments have suggested that the HydE substrate is a ubiquitous small molecule,[20, 51, 52] and only a limited collection of organisms have been identified that synthesize coenzyme M.[53] The observed reactivity with coenzyme M does however help define the size requirement and overall charge associated with the natural substrate. Taken together, our results support a hypothesis in which the natural substrate of HydE likely contains a functional group with partial or full negative charge at a distance of approximately 5 Å from a thiol. Also, given the nature of the effector molecules tested

coupled to the *in silico* docking results, the substrate is likely the size of a typical amino acid.

Potential role of SAM in HydE catalysis

The results reported herein provide evidence that *C. acetobutylicum* HydE purifies with a significant amount of SAM bound. The reduced purified enzyme exhibits two different EPR signals, both of which appear to arise from $[4Fe\text{-}4S]^{+}$ clusters; one of these signals overlays the signal observed for the SAM-bound state, suggesting that it is due to SAM that copurified with the enzyme. In addition, SAM cleavage assays in the absence of added SAM demonstrate the presence of SAM in the purified protein. The copurification of SAM, and by inference its high binding affinity, would be consistent with SAM serving as a cofactor rather than a cosubstrate during HydE catalysis. Alternatively, a high k_{on} rate for SAM binding could also be indicative of a mechanism utilizing two equivalents of SAM, where displacement of SAM cleavage products by SAM is required. Interestingly, other structurally similar radical SAM enzymes (BioB and LipA) also require multiple equivalents of SAM to accomplish their chemical reactions.[54, 55]

Mechanistic insights into HydE catalysis

If cysteine were the substrate for HydE, H-atom abstraction from the thiol would yield a thiyl radical that might subsequently undergo Cα-Cβ bond cleavage in a manner similar to the proposed mechanism for HydG.[56–58] Heterolytic cleavage of cysteine's Cα-Cβ bond would then produce a dehydroglycine fragment that would hydrolyze to glyoxylate; no glyoxylate is observed, however, in samples from SAM cleavage assays in the presence of cysteine (Figure S6). In the event of homolytic Cα-Cβ bond cleavage of cysteine, the reaction products would be thioformaldehyde ($S{=}CH_2$) and a glycyl radical; we have not yet been able to detect a glycyl radical nor its quenched product in assays. Following this latter possible reaction, two thioformaldehyde units could be joined by ammonia in a manner reminiscent of the *in vitro* synthesis of the DTMA bridge from the condensation of formaldehyde and ammonia.[59] The highly conserved region in the HydE structure that was found to bind thiocyanate could act as a second active site for this condensation to produce the DTMA bridge or as a temporary holding site for a DTMA precursor.[18] We have examined the effects of ammonia addition during HydE activity assays and have not observed stimulated dAdoH production (data not shown); this result is not unexpected given that ammonia may be reacting with thioformaldehyde at the bottom of the TIM barrel, some 13 Å away from the radical SAM cluster. Products of thiol lyase activity or intermediates in DTMA synthesis have not yet been detected by HPLC, LC/MS or spectroscopic methods, due presumably to the inherent difficulty in detecting these small, and in some cases reactive, molecules.

Intriguingly, the gene *aspA* that codes for aspartate ammonia-lyase is often associated within the *hydAEFG* operon (Figure 8 and S5), and could help increase the local concentration of ammonia during HydE catalysis. In addition to *aspA*, two other clusters of genomic neighbors that are involved in cysteine synthesis and metabolism are also often found near HydE in phylogenetically diverse organisms (Figure 8 and S5). These two enzyme nodes are both PLP-dependent, which may explain PLP's stimulatory effect observed in [FeFe]-

hydrogenase maturation assays.[60] Thioformaldehyde likely has a very short lifetime in a biological environment given its susceptibility to nucleophilic attack;[61] however, positioning ammonia (the putative source of the bridgehead atom) in the active site by the conserved carboxyl group of Glu58 and the side chain carbonyl group of Gln107 (*T. maritima* HydE numbering)[18] may promote the reaction with thioformaldehyde. The precedence for radical SAM enzymes generating small highly reactive molecules has been clearly made with HydG[11, 14] ThiH,[62] NocL/NosL,[58, 63] and NifB.[64]

Another potential candidate for the natural substrate of HydE is mercaptopyruvate. While mercaptopyruvate likely does not accumulate intracellularly as does cysteine[65], the enzymes cysteine transaminase and aspartate transaminase (both PLP-dependent enzymes) catalyze the production of mercaptopyruvate from cysteine.[66] This observation again provides a rational explanation for the reported stimulation of hydrogenase activity ten–fold with addition of PLP to cellular lysate assays.[60] Given the dramatic stimulation of SAM cleavage and D-atom incorporation by 3-mercaptopropionic acid, the potential for 3-MPA serving as a HydE substrate is also under investigation.

The radical SAM cartoon network (Figure 7A) shows that HydE is most closely related with PylB, HmdB, and BioB. It also shows similarity to CofG/CofH, MqnC/MqnE, and HydG/ThiH/3-Me; this network is a reflection of the degree of sequence and structural conservation among these enzymes and may translate mechanistically to HydE. Among these enzyme groups, it is intriguing that the CofG/CofH and HydG/ThiH/3-Me systems are involved in tyrosine and tryptophan Cα–βC bond cleavage events with the subsequent generation of glycine-like intermediate species.[25] Moreover, PylB has been proposed to generate a glycyl radical intermediate during conversion of lysine to methylornithine.[24] While the connections between HydE and MqnC/MqnE and HmdB are less clear, in part due to ambiguities regarding reactions catalyzed,[25] the striking similarity between PylB and HydE (Figure 7B) suggests the likelihood of mechanistic commonalities that may include similar substrates or intermediates. The structure of BioB also very closely resembles that of HydE, however BioB's sulfur insertion reaction depends upon the presence of a labile sulfur source from an auxiliary [2Fe-2S] cluster located ~5 Å from the substrate dethiobiotin.[18, 54, 67] Although HydE can have an auxiliary cluster, evidence indicates that this cluster is not essential for HydE function, arguing against BioB-like sulfur insertion chemistry. Collectively, these observations have led us to hypothesize that HydE DTMA synthesis may involve Cα–βC bond cleavage of a thiol containing molecule like cysteine to generate the reactive intermediate thioformaldehyde.

Concluding remarks

The observed effects of select low molecular mass thiols during HydE assays provide experimental insights into the putative mechanism and role of this enzyme during synthesis of the bridging DTMA ligand of the H-cluster. While this allows us to put together a more detailed description of how the H-cluster is built, several important issues must first be resolved before a final picture can be achieved. For example, the recent report of CN^- and CO-ligated iron species present on HydG during turnover, and the tracing of these to the 2Fe subcluster in HydA,[68] raises the question as to whether or not the sulfur atoms in the

bridging DTMA ligand arise from the accessory cluster in HydG and are transferred to HydF as part of the $Fe(CO)_2CN$ synthon.[68] In such a pathway, the product of HydE catalysis could stitch together two of the $Fe(CO)_2CN$–sulfide units to accomplish 2Fe subcluster formation on HydF. Alternatively, the sulfur of the DTMA ligand could come from an FeS cluster on HydF, and again be stitched together by the product of HydE catalysis.[13, 14] Another scenario, consistent with the importance of the thiol functional group suggested by the current work, involves sulfur being directly derived from the HydE substrate. Regardless of which mechanism is operative, the high binding affinity between HydE and HydF,[69] together with their existence as a *hydEF* fusion in some organisms,[8] suggests that HydE and HydF work closely together during H-cluster maturation. The current work provides important insights into the substrate of HydE and a potential mechanism for DTMA synthesis and will provide a critical foundation for further illumination of H-cluster assembly.

Supplementary Material

Refer to Web version on PubMed Central for supplementary material.

Acknowledgments

Funding Sources

The work reported herein was supported by the U.S. Department of Energy grant DE-FG02-10ER16194 (to J.B.B., J.W.P., and E.M.S.) and National Institutes of Health grants R01 GM60595 and U54 GM093342 (to P.C.B.)

JNB was supported by the United States Air Force Academy Faculty Pipeline PhD Program. We thank Brian Bothner and Jonathan Hilmer of the MSU Mass Spectrometry Facility for assistance and advice on MS experiments, and Sunil Ojha for fruitful discussions.

ABBREVIATIONS

βME	β-mercaptoethanol
CoA	coenzyme A
CoM	coenzyme M
dAdo•	5’deoxyadenosyl radical
dAdoH	5’-deoxyadenosine
DRF	5-deazariboflavin
DTT	dithiothreitol
DTMA	dithiomethylamine
EPR	electron paramagnetic resonance
GSH	glutathione
HEPES	2-[4-(2-hydroxyethyl)piperazin-1-yl]ethanesulfonic acid
HPLC	high pressure liquid chromatography

IPTG	isopropyl β-D-1-thiogalactopyranoside
LC/MS	liquid chromatography mass spectrometry
L-Hcy	L-homocysteine
LMCT	ligand to metal charge transfer
MP	mercaptopyruvate
MTA	methylthioadenosine
PLP	pyridoxal-phosphate
PMSF	phenylmethylsulfonyl fluoride
SAM	*S*-adenosyl-L-methionine
SFLD	Structure Function Linkage Database
SSN	sequence similarity network
TIM	triosephosphosphate isomerase
γGC	γ-L-glutamyl-L-cysteine
3-MPA	3-mercaptopropionic acid

REFERENCES

1. Peters JW. Structure and mechanism of iron-only hydrogenases. Curr. Opin. Struct. Biol. 1999; 9:670–676. [PubMed: 10607666]
2. Madden C, Vaughn MD, Diez-Perez I, Brown KA, King PW, Gust D, Moore AL, Moore TA. Catalytic Turnover of [FeFe]-Hydrogenase Based on Single-Molecule Imaging. Journal of the American Chemical Society. 2012; 134:1577–1582. [PubMed: 21916466]
3. Fritsch J, Scheerer P, Frielingsdorf S, Kroschinsky S, Friedrich B, Lenz O, Spahn CMT. The crystal structure of an oxygen-tolerant hydrogenase uncovers a novel iron-sulphur centre. Nature. 2011; 479:U249–U134.
4. Stripp ST, Goldet G, Brandmayr C, Sanganas O, Vincent KA, Haumann M, Armstrong FA, Happe T. How oxygen attacks [FeFe] hydrogenases from photosynthetic organisms. Proceedings of the National Academy of Sciences of the United States of America. 2009; 106:17331–17336. [PubMed: 19805068]
5. Adams MWW. The Mechanisms of H-2 Activation and Co Binding by Hydrogenase-I and Hydrogenase-Ii of Clostridium-Pasteurianum. Journal of Biological Chemistry. 1987; 262:15054–15061. [PubMed: 2822711]
6. Hagen WR, Vanberkelarts A, Krusewolters KM, Voordouw G, Veeger C. The Iron-Sulfur Composition of the Active-Site of Hydrogenase from Desulfovibrio-Vulgaris (Hildenborough) Deduced from Its Subunit Structure and Total Iron-Sulfur Content. FEBS letters. 1986; 203:59–63.
7. Nicolet Y, Piras C, Legrand P, Hatchikian CE, Fontecilla-Camps JC. Desulfovibrio desulfuricans iron hydrogenase: the structure shows unusual coordination to an active site Fe binuclear center. Structure. 1999; 7:13–23. [PubMed: 10368269]
8. Posewitz MC, King PW, Smolinski SL, Zhang L, Seibert M, Ghirardi ML. Discovery of two novel radical S-adenosylmethionine proteins required for the assembly of an active [Fe] hydrogenase. J. Biol. Chem. 2004; 279:25711–25720. [PubMed: 15082711]
9. Rubach JK, Brazzolotto X, Gaillard J, Fontecave M. Biochemical characterization of the HydE and HydG iron-only hydrogenase maturation enzymes from Thermatoga maritima. FEBS Lett. 2005; 579:5055–5060. [PubMed: 16137685]

10. Pilet E, Nicolet Y, Mathevon C, Douki T, Fontecilla-Camps JC, Fontecave M. The role of the maturase HydG in [FeFe]-hydrogenase active site synthesis and assembly. FEBS Lett. 2009; 583:506–511. [PubMed: 19166853]
11. Driesener RC, Challand MR, McGlynn SE, Shepard EM, Boyd ES, Broderick JB, Peters JW, Roach PL. [FeFe]-hydrogenase cyanide ligands derived from S-adenosylmethionine-dependent cleavage of tyrosine. Angewandte Chemie. 2010; 49:1687–1690. [PubMed: 20108298]
12. Shepard EM, Duffus BR, George SJ, McGlynn SE, Challand MR, Swanson KD, Roach PL, Cramer SP, Peters JW, Broderick JB. [FeFe]-hydrogenase maturation: HydG-catalyzed synthesis of carbon monoxide. Journal of the American Chemical Society. 2010; 132:9247–9249. [PubMed: 20565074]
13. Shepard EM, Mus F, Betz JN, Byer AS, Duffus BR, Peters JW, Broderick JB. [FeFe]-Hydrogenase Maturation. Biochemistry. 2014
14. Shepard EM, McGlynn SE, Bueling AL, Grady-Smith CS, George SJ, Winslow MA, Cramer SP, Peters JW, Broderick JB. Synthesis of the 2Fe subcluster of the [FeFe]-hydrogenase H cluster on the HydF scaffold. Proceedings of the National Academy of Sciences of the United States of America. 2010; 107:10448–10453. [PubMed: 20498089]
15. Brazzolotto X, Rubach JK, Gaillard J, Gambarelli S, Atta M, Fontecave M. The [Fe-Fe]-hydrogenase maturation protein HydF from Thermotoga maritima is a GTPase with an iron-sulfur cluster. J. Biol. Chem. 2006; 281:769–774. [PubMed: 16278209]
16. Czech I, Silakov A, Lubitz W, Happe T. The [FeFe]-hydrogenase maturase HydF from Clostridium acetobutylicum contains a CO and CN- ligated iron cofactor. FEBS letters. 2010; 584:638–642. [PubMed: 20018187]
17. Berggren G, Adamska A, Lambertz C, Simmons TR, Esselborn J, Atta M, Gambarelli S, Mouesca JM, Reijerse E, Lubitz W, Happe T, Artero V, Fontecave M. Biomimetic assembly and activation of [FeFe]-hydrogenases. Nature. 2013; 499:66–69. [PubMed: 23803769]
18. Nicolet Y, Rubach JK, Posewitz MC, Amara P, Mathevon C, Atta M, Fontecave M, Fontecilla-Camps JC. X-ray structure of the [FeFe]-hydrogenase maturase HydE from Thermotoga maritima. J. Biol. Chem. 2008; 283:18861–18872. [PubMed: 18400755]
19. Nicolet Y, Amara P, Mouesca JM, Fontecilla-Camps JC. Unexpected electron transfer mechanism upon AdoMet cleavage in radical SAM proteins. Proceedings of the National Academy of Sciences of the United States of America. 2009; 106:14867–14871. [PubMed: 19706452]
20. McGlynn SE, Shepard EM, Winslow MA, Naumov AV, Duschene KS, Posewitz MC, Broderick WE, Broderick JB, Peters JW. HydF as a scaffold protein in [FeFe] hydrogenase H-cluster biosynthesis. FEBS Lett. 2008; 582:2183–2187. [PubMed: 18501709]
21. Broderick JB, Byer AS, Duschene KS, Duffus BR, Betz JN, Shepard EM, Peters JW. H-Cluster assembly during maturation of the [FeFe]-hydrogenase. Journal of biological inorganic chemistry : JBIC : a publication of the Society of Biological Inorganic Chemistry. 2014
22. Nicolet Y, Fontecilla-Camps JC. Structure-Function Relationships in [FeFe]-Hydrogenase Active Site Maturation. Journal of Biological Chemistry. 2012; 287:13532–13540. [PubMed: 22389497]
23. Myers WK, Stich TA, Suess DL, Kuchenreuther JM, Swartz JR, Britt RD. The Cyanide Ligands of [FeFe] Hydrogenase: Pulse EPR Studies of (13)C and (15)N-Labeled H-Cluster. Journal of the American Chemical Society. 2014; 136:12237–12240. [PubMed: 25133957]
24. Quitterer F, List A, Eisenreich W, Bacher A, Groll M. Crystal structure of methylornithine synthase (PylB): insights into the pyrrolysine biosynthesis. Angewandte Chemie. 2012; 51:1339–1342. [PubMed: 22095926]
25. Broderick JB, Duffus BR, Duschene KS, Shepard EM. Radical s-adenosylmethionine enzymes. Chemical reviews. 2014; 114:4229–4317. [PubMed: 24476342]
26. Betz, JN.; Shepard, EM.; Broderick, JB. Radical SAM Enzymes and Their Roles in Complex Cluster Assembly. In: Goddard, WA., III; Cho, AE., editors. Metalloproteins: Theory, Calculations, and Experiments. CRC Press; 2015. (in press)
27. Fish WW. Rapid colorimetric micromethod for the quantitation of complexed iron in biological samples. Methods Enzymol. 1988; 158:357–364. [PubMed: 3374387]
28. Duschene KS, Broderick JB. The antiviral protein viperin is a radical SAM enzyme. FEBS letters. 2010; 584:1263–1267. [PubMed: 20176015]

29. Stoll S, Schweiger A. EasySpin, a comprehensive software package for spectral simulation and analysis in EPR. J Magn Reson. 2006; 178:42–55. [PubMed: 16188474]
30. Walsby CJ, Ortillo D, Broderick WE, Broderick JB, Hoffman BM. An anchoring role for FeS clusters: chelation of the amino acid moiety of S-adenosylmethionine to the unique iron site of the [4Fe-4S] cluster of pyruvate formate-lyase activating enzyme. Journal of the American Chemical Society. 2002; 124:11270–11271. [PubMed: 12236732]
31. Morris GM, Huey R, Lindstrom W, Sanner MF, Belew RK, Goodsell DS, Olson AJ. AutoDock4 and AutoDockTools4: Automated Docking with Selective Receptor Flexibility. J Comput Chem. 2009; 30:2785–2791. [PubMed: 19399780]
32. Hanwell MD, Curtis DE, Lonie DC, Vandermeersch T, Zurek E, Hutchison GR. Avogadro: an advanced semantic chemical editor, visualization, and analysis platform. J Cheminformatics. 2012; 4
33. Database, SFL. Radical SAM Superfamily. San Francisco: University of California; 2014.
34. Zhao S, Sakai A, Zhang X, Vetting MW, Kumar R, Hillerich B, San Francisco B, Solbiati J, Steves A, Brown S, Akiva E, Barber A, Seidel RD, Babbitt PC, Almo SC, Gerlt JA, Jacobson MP. Prediction and characterization of enzymatic activities guided by sequence similarity and genome neighborhood networks. eLife. 2014:e03275.
35. Leinonen R, Akhtar R, Birney E, Bower L, Cerdeno-Tarraga A, Cheng Y, Cleland I, Faruque N, Goodgame N, Gibson R, Hoad G, Jang M, Pakseresht N, Plaister S, Radhakrishnan R, Reddy K, Sobhany S, Ten Hoopen P, Vaughan R, Zalunin V, Cochrane G. The European Nucleotide Archive. Nucleic Acids Res. 2011; 39:D28–D31. [PubMed: 20972220]
36. Barber AE 2nd, Babbitt PC. Pythoscape: a framework for generation of large protein similarity networks. Bioinformatics. 2012; 28:2845–2846. [PubMed: 22962345]
37. UniProt, C. Activities at the Universal Protein Resource (UniProt). Nucleic Acids Res. 2014; 42:D191–D198. [PubMed: 24253303]
38. Shen G, Balasubramanian R, Wang T, Wu Y, Hoffart LM, Krebs C, Bryant DA, Golbeck JH. SufR coordinates two [4Fe-4S]2+, 1+ clusters and functions as a transcriptional repressor of the sufBCDS operon and an autoregulator of sufR in cyanobacteria. The Journal of biological chemistry. 2007; 282:31909–31919. [PubMed: 17827500]
39. Wecksler SR, Stoll S, Tran H, Magnusson OT, Wu SP, King D, Britt RD, Klinman JP. Pyrroloquinoline quinone biogenesis: demonstration that PqqE from Klebsiella pneumoniae is a radical S-adenosyl-L-methionine enzyme. Biochemistry. 2009; 48:10151–10161. [PubMed: 19746930]
40. Ruzicka FJ, Frey PA. Glutamate 2,3-aminomutase: a new member of the radical SAM superfamily of enzymes. Biochimica et biophysica acta. 2007; 1774:286–296. [PubMed: 17222594]
41. Broderick JB, Henshaw TF, Cheek J, Wojtuszewski K, Smith SR, Trojan MR, McGhan RM, Kopf A, Kibbey M, Broderick WE. Pyruvate formate-lyase-activating enzyme: Strictly anaerobic isolation yields active enzyme containing a [3Fe-4S](+) cluster. Biochemical and biophysical research communications. 2000; 269:451–456. [PubMed: 10708574]
42. Rupp H, Rao KK, Hall DO, Cammack R. Electron spin relaxation of iron-sulphur proteins studied by microwave power saturation. Biochim. Biophys. Acta. 1978; 537:255–269. [PubMed: 215217]
43. Kuchenreuther JM, Stapleton JA, Swartz JR. Tyrosine, cysteine, and S-adenosyl methionine stimulate in vitro [FeFe] hydrogenase activation. PLoS.One. 2009; 4:e7565. [PubMed: 19855833]
44. Chatterjee A, Hazra AB, Abdelwahed S, Hilmey DG, Begley TP. A "Radical Dance" in Thiamin Biosynthesis: Mechanistic Analysis of the Bacterial Hydroxymethylpyrimidine Phosphate Synthase. Angew Chem Int Edit. 2010; 49:8653–8656.
45. Tang LH, Su M, Chi LY, Zhang JL, Zhang HH, Zhu L. Residue Val237 is critical for the enantioselectivity of Penicillium expansum lipase. Biotechnol Lett. 2014; 36:633–639. [PubMed: 24338160]
46. Stone CL, Hurley TD, Peggs CF, Kedishvili NY, Davis GJ, Thomasson HR, Li TK, Bosron WF. Cimetidine Inhibition of Human Gastric and Liver Alcohol-Dehydrogenase Isoenzymes - Identification of Inhibitor Complexes by Kinetics and Molecular Modeling. Biochemistry. 1995; 34:4008–4014. [PubMed: 7696266]

47. Stoddard BL, Koshland DE. Prediction of the Structure of a Receptor Protein Complex Using a Binary Docking Method. Nature. 1992; 358:774–776. [PubMed: 1324436]
48. Peters JW, Szilagyi RK, Naumov A, Douglas T. A radical solution for the biosynthesis of the H-cluster of hydrogenase. FEBS Lett. 2006; 580:363–367. [PubMed: 16386249]
49. Ashburner M, Ball CA, Blake JA, Botstein D, Butler H, Cherry JM, Davis AP, Dolinski K, Dwight SS, Eppig JT, Harris MA, Hill DP, Issel-Tarver L, Kasarskis A, Lewis S, Matese JC, Richardson JE, Ringwald M, Rubin GM, Sherlock G. Gene ontology: tool for the unification of biology. The Gene Ontology Consortium. Nature genetics. 2000; 25:25–29. [PubMed: 10802651]
50. Nicolet Y, Rohac R, Martin L, Fontecilla-Camps JC. X-ray snapshots of possible intermediates in the time course of synthesis and degradation of protein-bound Fe4S4 clusters. Proceedings of the National Academy of Sciences of the United States of America. 2013; 110:7188–7192. [PubMed: 23596207]
51. King PW, Posewitz MC, Ghirardi ML, Seibert M. Functional studies of [FeFe] hydrogenase maturation in an Escherichia coli biosynthetic system. Journal of bacteriology. 2006; 188:2163–2172. [PubMed: 16513746]
52. McGlynn SE, Ruebush SS, Naumov A, Nagy LE, Dubini A, King PW, Broderick JB, Posewitz MC, Peters JW. In vitro activation of [FeFe] hydrogenase: new insights into hydrogenase maturation. J. Biol. Inorg. Chem. 2007; 12:443–447. [PubMed: 17372774]
53. Balch WE, Wolfe RS. Specificity and Biological Distribution of Coenzyme M (2-Mercaptoethanesulfonic Acid). Journal of bacteriology. 1979; 137:256–263. [PubMed: 104960]
54. Fugate CJ, Stich TA, Kim EG, Myers WK, Britt RD, Jarrett JT. 9-Mercaptodethiobiotin Is Generated as a Ligand to the [2Fe-2S](+) Cluster during the Reaction Catalyzed by Biotin Synthase from Escherichia coli. Journal of the American Chemical Society. 2012
55. Douglas P, Kriek M, Bryant P, Roach PL. Lipoyl synthase inserts sulfur atoms into an octanoyl substrate in a stepwise manner. Angew Chem Int Edit. 2006; 45:5197–5199.
56. Kuchenreuther JM, Myers WK, Stich TA, George SJ, Nejatyjahromy Y, Swartz JR, Britt RD. A radical intermediate in tyrosine scission to the CO and CN- ligands of FeFe hydrogenase. Science. 2013; 342:472–475. [PubMed: 24159045]
57. Duffus BR, Ghose S, Peters JW, Broderick JB. Reversible H Atom Abstraction Catalyzed by the Radical S-Adenosylmethionine Enzyme HydG. Journal of the American Chemical Society. 2014
58. Nicolet Y, Zeppieri L, Amara P, Fontecilla-Camps JC. Crystal Structure of Tryptophan Lyase (NosL): Evidence for Radical Formation at the Amino Group of Tryptophan. Angewandte Chemie. 2014
59. Li HX, Rauchfuss TB. Iron carbonyl sulfides, formaldehyde, and amines condense to give the proposed azadithiolate cofactor of the Fe-only hydrogenases. Journal of the American Chemical Society. 2002; 124:726–727. [PubMed: 11817928]
60. Kuchenreuther JM, Britt RD, Swartz JR. New insights into [FeFe] hydrogenase activation and maturase function. PloS one. 2012; 7:e45850. [PubMed: 23049878]
61. Johnson DR, Powell FX, Kirchhof Wh. Microwave Spectrum, Ground State Structure, and Dipole Moment of Thioformaldehyde. J Mol Spectrosc. 1971; 39:136-&.
62. Kriek M, Martins F, Challand MR, Croft A, Roach PL. Thiamine biosynthesis in Escherichia coli: identification of the intermediate and by-product derived from tyrosine. Angew. Chem. Int. Ed Engl. 2007; 46:9223–9226. [PubMed: 17969213]
63. Zhang Q, Li YX, Chen DD, Yu Y, Duan LA, Shen B, Liu W. Radical-mediated enzymatic carbon chain fragmentation-recombination. Nature chemical biology. 2011; 7:154–160. [PubMed: 21240261]
64. Wiig JA, Hu YL, Lee CC, Ribbe MW. Radical SAM-Dependent Carbon Insertion into the Nitrogenase M-Cluster. Science. 2012; 337:1672–1675. [PubMed: 23019652]
65. Ogony J, Mare S, Wu W, Ercal N. High performance liquid chromatography analysis of 2-mercaptoethylamine (cysteamine) in biological samples by derivatization with N-(1-pyrenyl) maleimide (NPM) using fluorescence detection. J Chromatogr B. 2006; 843:57–62.
66. Nagahara N, Sawada N. The mercaptopyruvate pathway in cysteine catabolism: A physiologic role and related disease of the multifunctional 3-mercaptopyruvate sulfurtransferase. Curr Med Chem. 2006; 13:1219–1230. [PubMed: 16719781]

67. Berkovitch F, Nicolet Y, Wan JT, Jarrett JT, Drennan CL. Crystal structure of biotin synthase, an S-adenosylmethionine-dependent radical enzyme. Science. 2004; 303:76–79. [PubMed: 14704425]

68. Kuchenreuther JM, Myers WK, Suess DLM, Stich TA, Pelmenschikov V, Shiigi SA, Cramer SP, Swartz JR, Britt RD, George SJ. The HydG Enzyme Generates an Fe(CO)(2)(CN) Synthon in Assembly of the FeFe Hydrogenase H-Cluster. Science. 2014; 343:424–427. [PubMed: 24458644]

69. Vallese F, Berto P, Ruzzene M, Cendron L, Sarno S, De Rosa E, Giacometti GM, Costantini P. Biochemical Analysis of the Interactions between the Proteins Involved in the [FeFe]-Hydrogenase Maturation Process. Journal of Biological Chemistry. 2012; 287:36544–36555. [PubMed: 22932901]

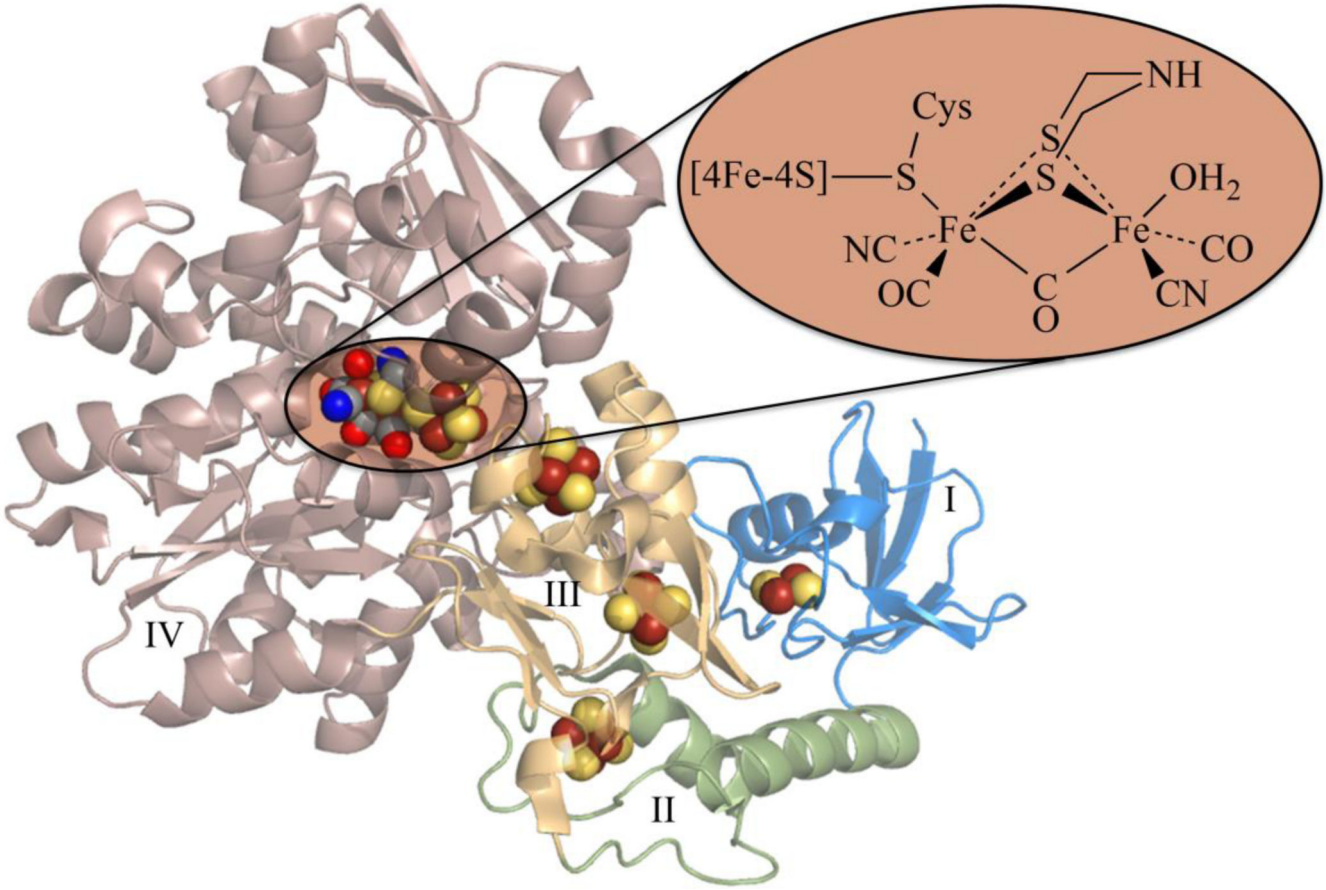

Figure 1.

[FeFe]-hydrogenase crystal structure with H-cluster. The active site is located in domain IV common to all [FeFe]-hydrogenases. Atoms explicitly drawn have the following color scheme: Iron-brown, Sulfur-yellow, Nitrogen-blue, Oxygen-Red, and Carbon-gray. PDB ID: 3C8Y.

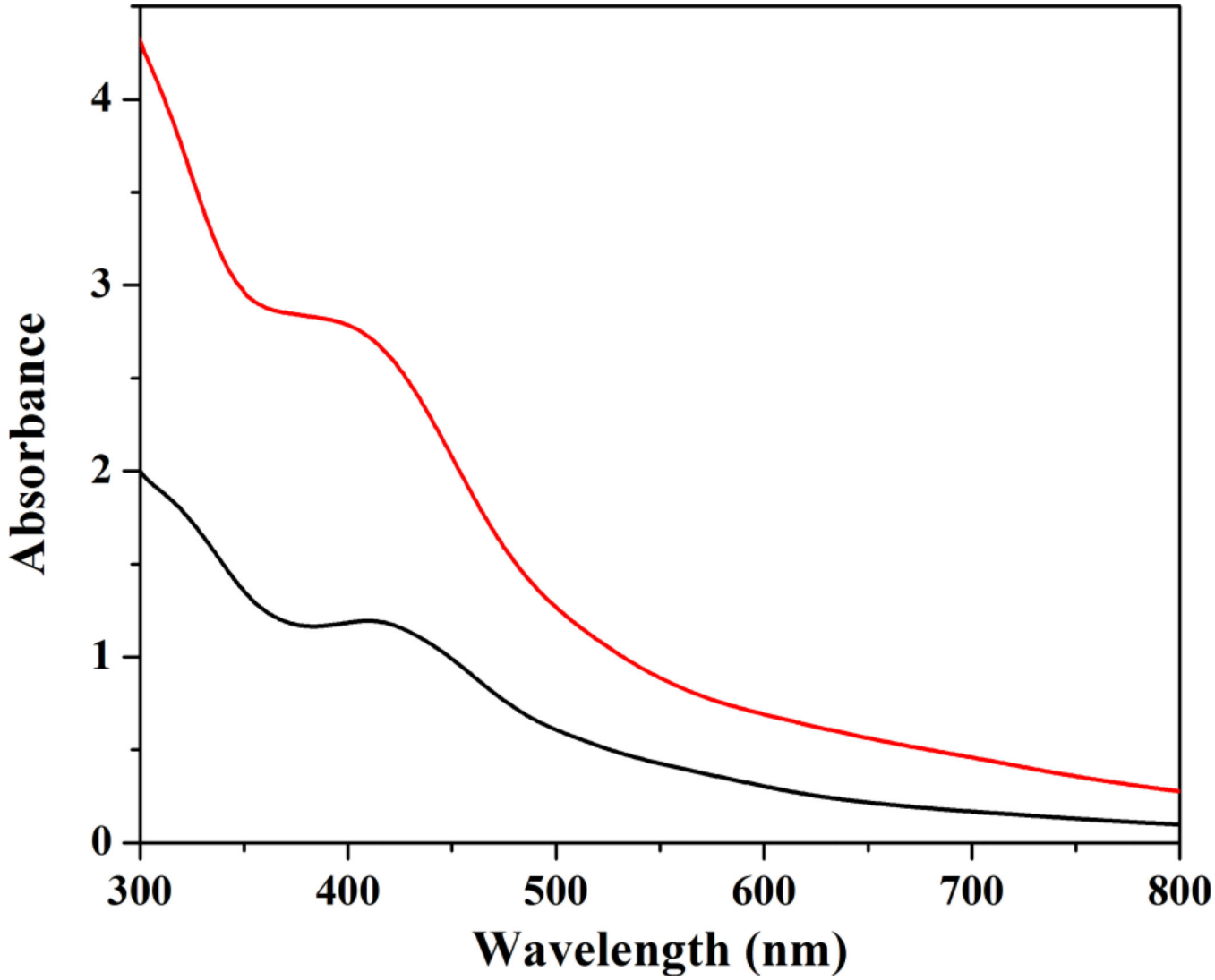

Figure 2.

UV-Vis spectra of *C. acetobutylicum* HydE as-purified (black) and following chemical reconstitution (red). Protein concentrations adjusted to 83.4 μM. As-purified and reconstituted protein contained 3.7 +/− 0.1 and 8.6 +/− 0.1 Fe/protein respectively.

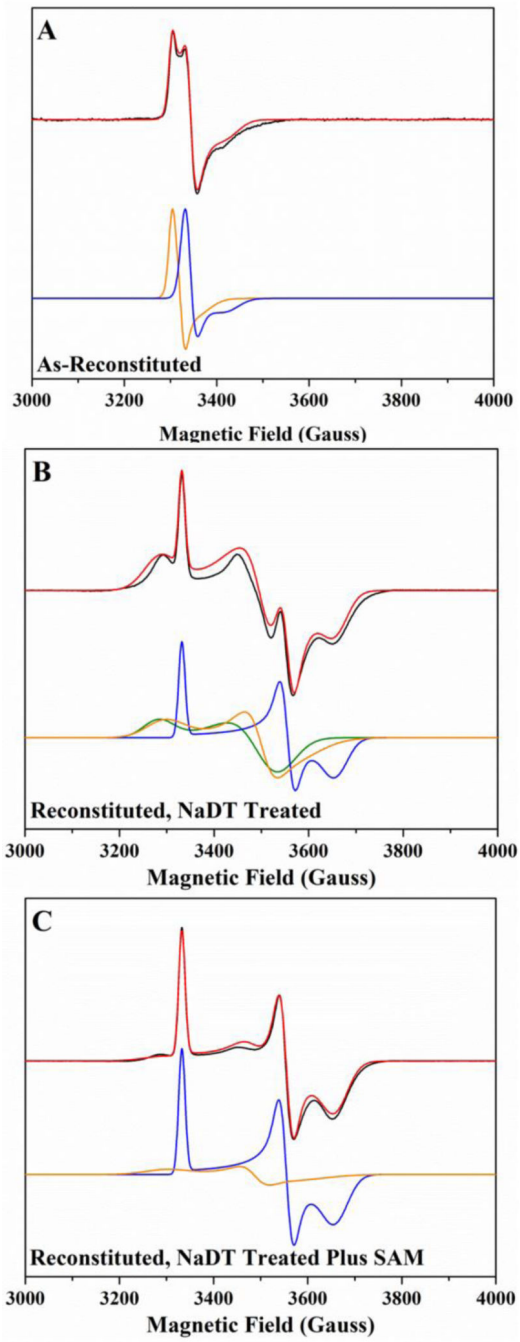

Figure 3.

Low temperature EPR spectra of *C. acetobutylicum* HydE. (A) As-reconstituted enzyme. (B) Dithionite reduced enzyme. (C) Dithionite reduced enzyme plus exogenous SAM. All spectra were collected at 12 K with 275 μM chemically reconstituted HydE containing 7.6 ± 0.1 Fe/protein. In all panels, the experimental data traces appear in black and are overlaid with the composite simulation traces (shown in red, see below). In panel A, the simulated traces for cluster 1 and cluster 2 are depicted in orange and blue, respectively. In panel B, the simulated trace for the N-terminal cluster appears in green, while the simulated trace for the

C-terminal cluster is shown in orange; the blue simulated trace represents the SAM coordinated form of the N-terminal cluster. In panel C, the blue trace again represents the SAM coordinated form of the N-terminal cluster, while the orange trace depicts the C-terminal cluster.

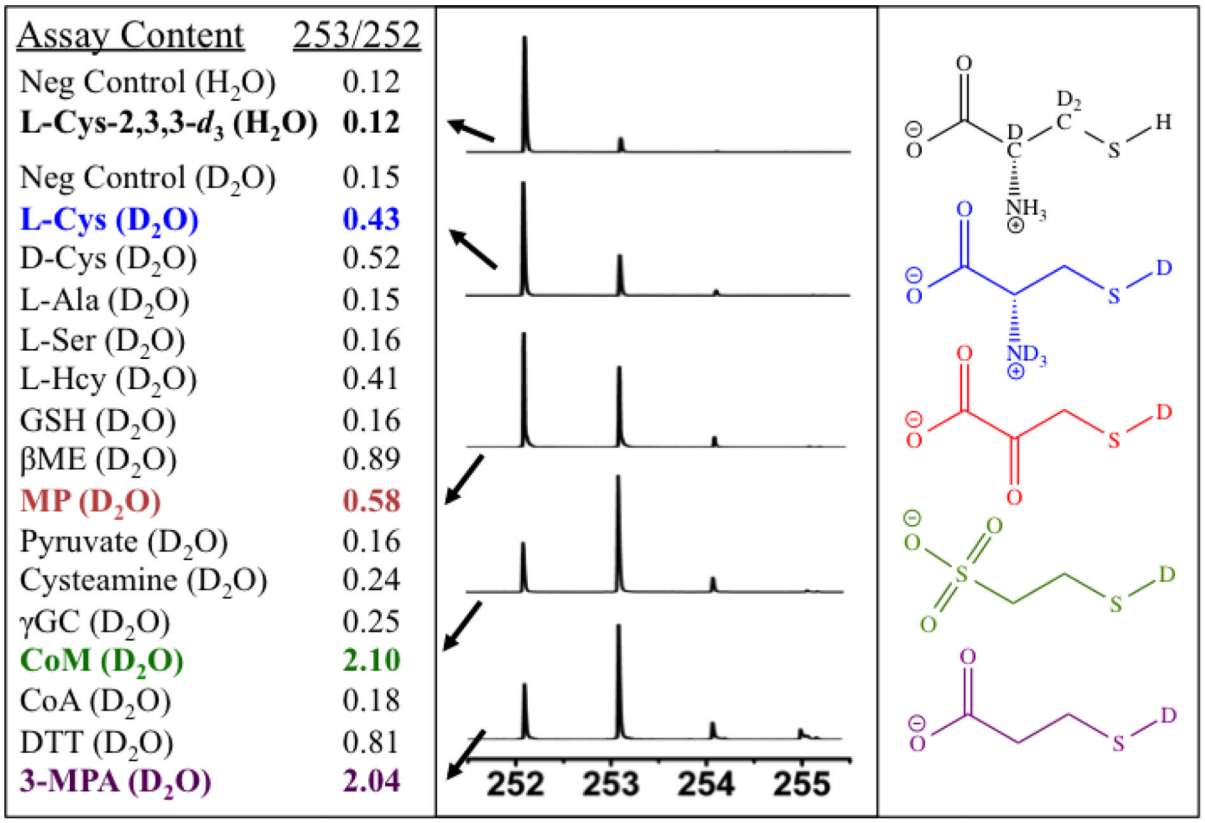

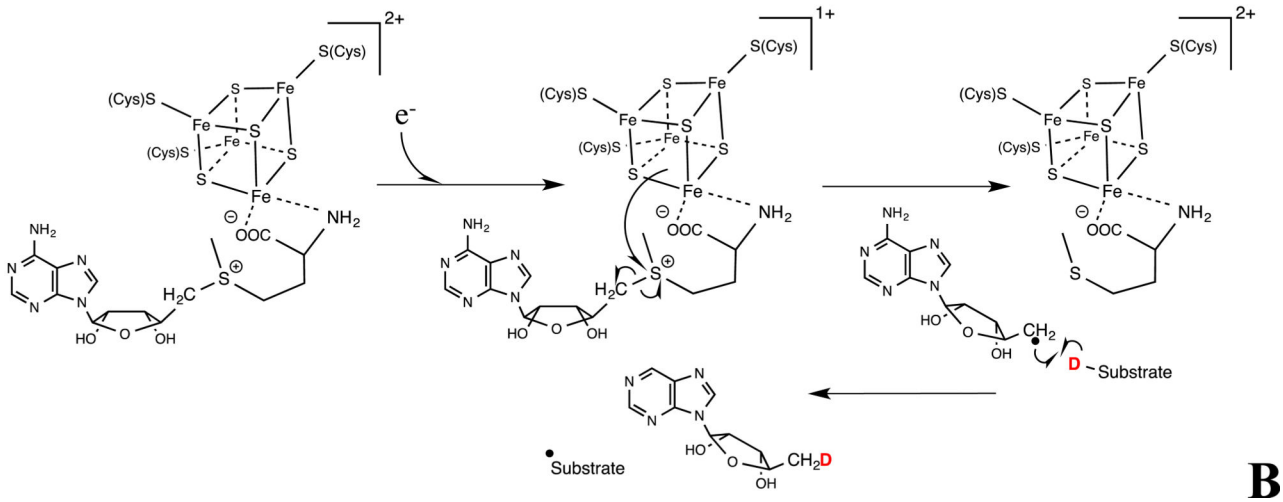

Figure 4.

(A) Results of analysis for deuterium incorporation into product 5'-deoxyadenosine after assay of HydE with a range of small molecules in D_2O buffer. Mass spectroscopic result for dAdo(H/D) from selected assays are shown on the right, and the ratio of mass peak ratios are shown on left. B. Initial steps in a radical SAM reaction that can lead to D-atom incorporation into dAdo.

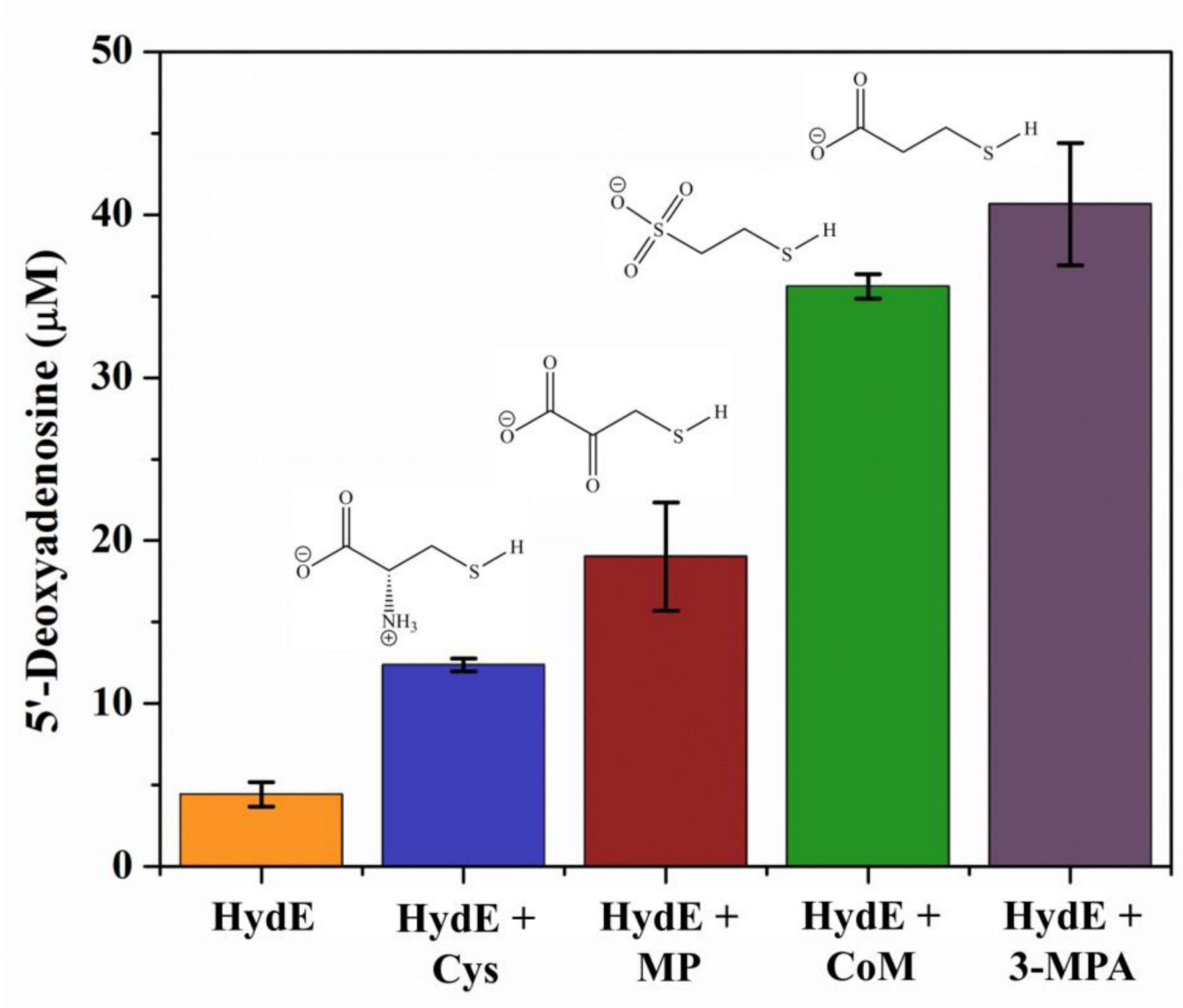

Figure 5.

Stimulation of 5-deoxyadenosine production by addition of L-Cys, mercaptopyruvate, and coenzyme M (2.5 mM) to a HydE (25 μM) / SAM (500 μM) assay. Assays were quenched after 30 minutes of reaction.

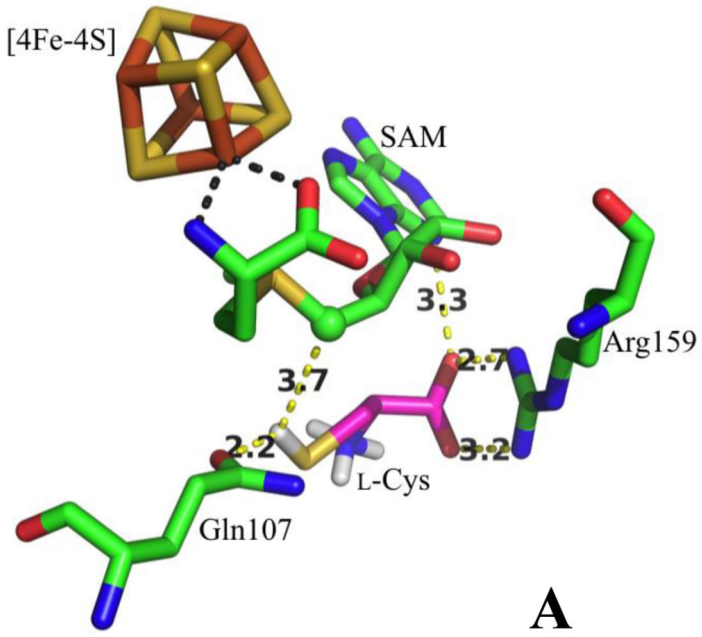

Docked Molecules	Binding Energy (kJ/mol)
γGC	-7.0
Mercaptopyruvate	-5.0
Coenzyme M	-4.7
L-Homocysteine	-4.7
Pyruvate	-4.7
L-Alanine	-4.3
L-Cysteine	-4.3
DTT	-3.9
L-Serine	-3.8
Cysteamine	-3.7
D-Cys	-3.7
β-ME	-3.0
CoA	5.8

B

Figure 6.

(A) Active site of *T. maritima* HydE with [4Fe-4S] cluster, SAM, Arg159, Gln107, and L-Cys from in silico modeling. L-cysteine in purple represents the location of the other thiols all in their lowest energy binding conformation. The deoxyadenosyl radical's unpaired electron that abstracts the H/D-atom from substrates is generated on the 5' carbon of SAM (green sphere). This carbon is at distances to the sulfur atom of the mercaptans comparable to those of other radical SAM enzymes with crystal structures solved with SAM and substrates.[13] All distances are in Å. Color Scheme unless otherwise noted: carbon (green), oxygen (red), nitrogen (blue), iron (orange), and sulfur (yellow). PDB ID: 3IIZ. (B) Relative binding energies of molecules from in silico docking experiments.

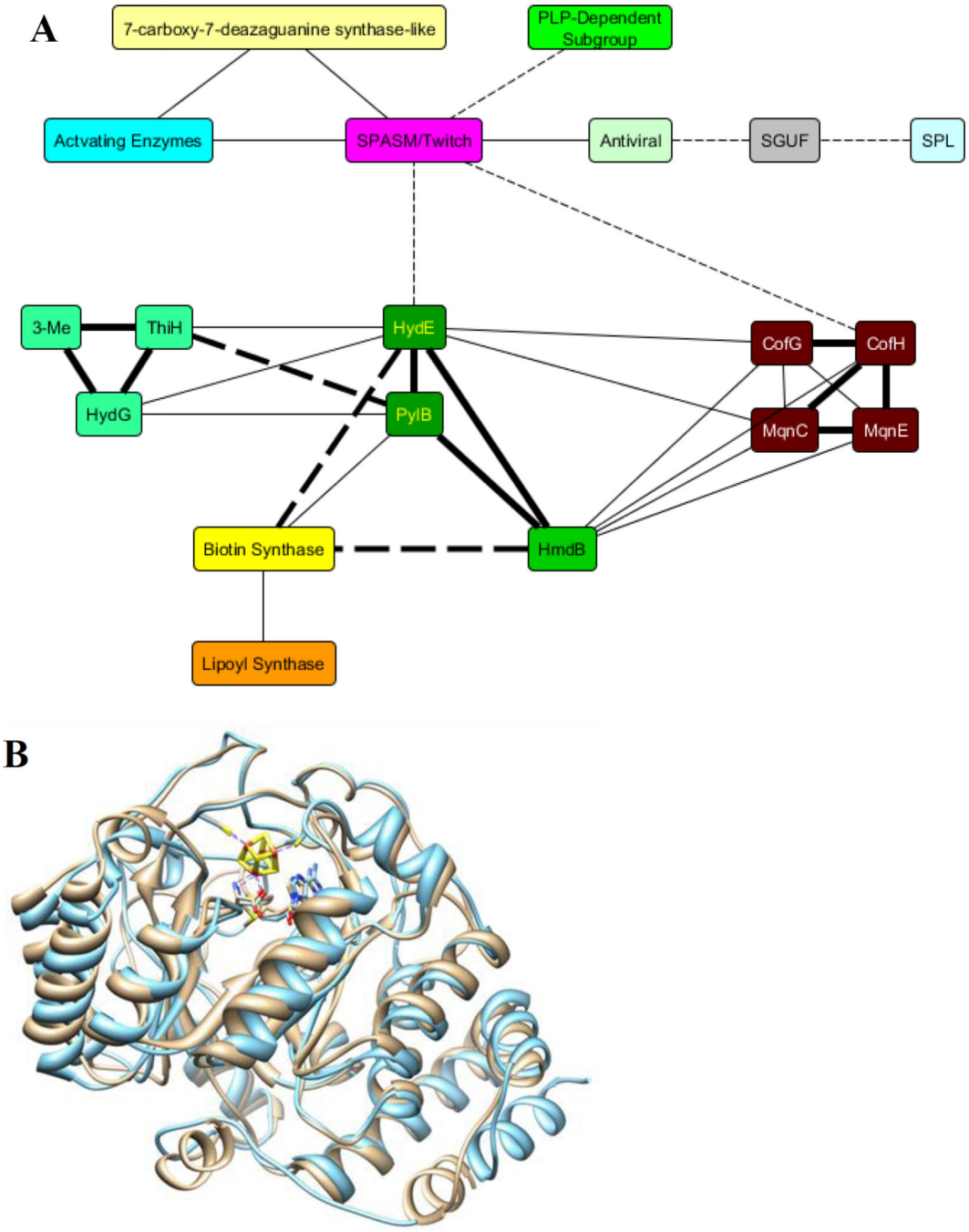

Figure 7.

(A) Cartoon network representing the relationship of HydE family sequences to other well characterized subgroups and families described in the SFLD. The thick lines represent a higher degree of relatedness that thin lines and the unbroken lines along with the same colored boxes represent membership of the same subgroup. The thin, broken lines represent a more distant relationship. No information is inferred by the lengths of the edges. The "Antiviral" node includes Viperin, 3-Me includes NosL/NocL the tryptophan lyases, and SGUF denotes a subgroup of radical SAM enzymes with unknown function. (B) Overlay of

PylB (PDB ID: 3T7V) shown in tan and HydE (PDB ID: 3CIW) shown in blue crystal structures.

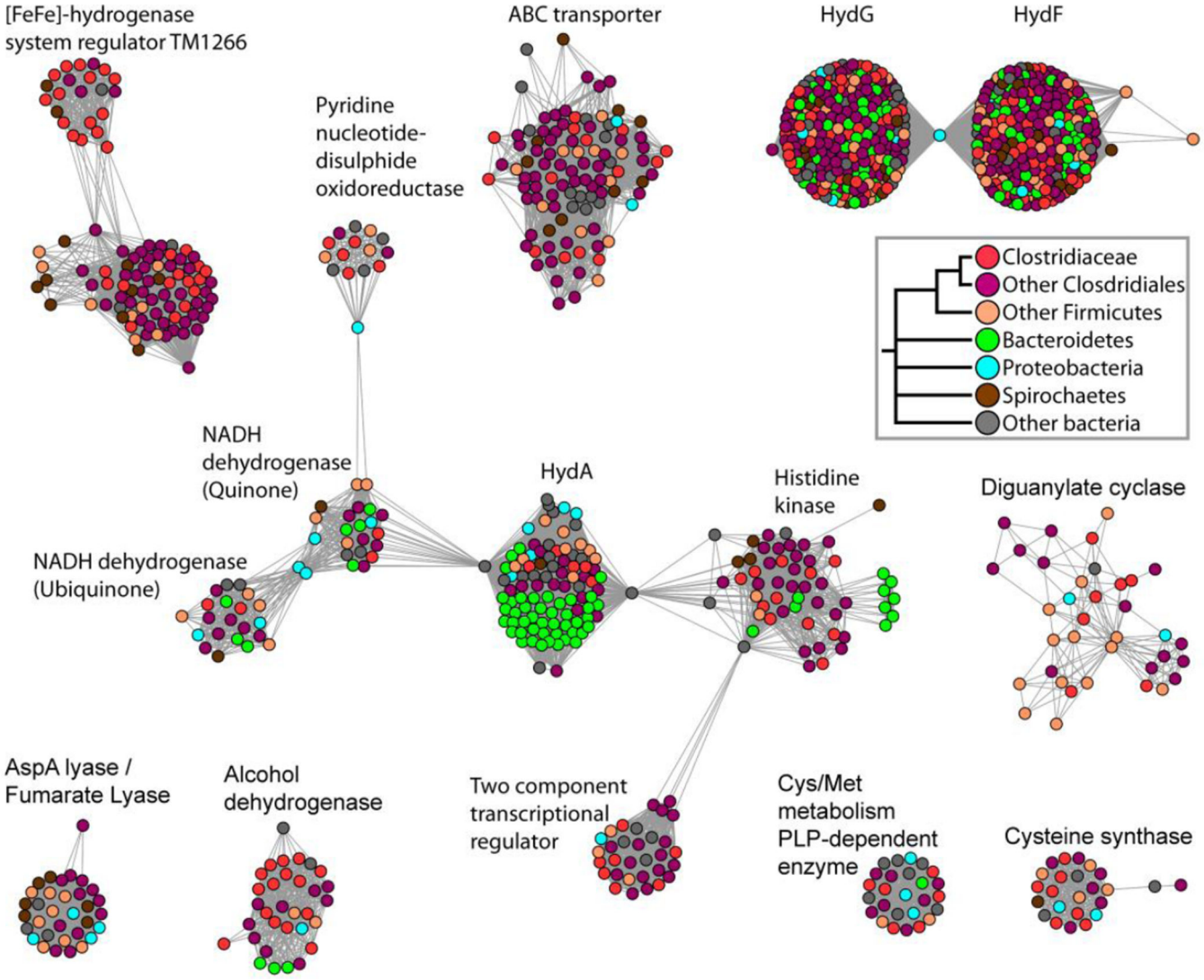

Figure 8.

A bridged genomic context network for HydE enzymes. Circles represent genomic neighbors within 10 genes upstream/downstream of the 563 HydE enzymes as classified by the SFLD. Connections represent BLAST pairwise sequence similarity with E-value more significant than $1e^{-20}$. The 1,054 proteins are clustered into sets of similar sequences that are visually identifiable. Only clusters that could be assigned with function are shown and accompanied with the relevant titles. Colors represent the phylogenetic origin of the organisms in which enzymes are encoded, as shown in the legend. Clusters are roughly ordered by size and heterogeneous phylogenetic origin (from upper left to lower right). The largest and most phylogenetically diverse clusters are enriched with functions that typify the H cluster biosynthesis pathways, such as HydA, HydF, HydG and TM1266 proteins, strengthening our confidence in the ability of this method to capture biologically relevant signals.